Available online at www.sciencedirect.com
ScienceDirect
Journal of Nuclear Materials 363–365 (2007) 330–334
journal of nuclear materials
www.elsevier.com/locate/jnucmat

# B2-EIRENE simulation of plasma and neutrals in MAGNUM-PSI

M. Baeva [a,*], W.J. Goedheer [a], N.J. Lopes Cardozo [a], D. Reiter [b]

[a] *FOM-Institute for Plasma Physics Rijnhuizen, P.O. Box 1207, 3430 BE Nieuwegein, The Netherlands*
[b] *Institut fuer Plasmaphysik, Association EURATOM, TEC, FZ-Juelich, Germany*

**Abstract**

A self-consistent description (performed by means of the B2-EIRENE code package) of a hydrogen plasma including electrons, ions and neutral background gas is used to investigate the processes and plasma behavior under conditions expected in MAGNUM-PSI. Several cases varying in gas-puffing, pumping rate, and plasma parameters are simulated. In all cases a detached plasma regime is achieved. The plasma density increases considerably for higher neutral pressures up to $(1–5) \times 10^{14}\ cm^{-3}$. The particle flux to the target is $\sim 10^{24}\ m^{-2}\ s^{-1}$ and the plasma heat flux is $\sim 10\ MW\ m^{-2}$. The latter is significantly reduced in front of the target due to electron and ion cooling resulting from ionization and dissociation of $H_2$ molecules, and charge exchange/elastic collisions. Under the conditions of investigation, the losses due to molecule activated recombination are dominant compared with 3-body recombination of atomic ions.


*PACS:* 52.65

*Keywords:* B2-EIRENE code; Simulation; Hydrogen; Detached plasma

## 1. Introduction

The linear device MAGNUM-PSI, which is currently under construction, is aimed at the study of plasma surface interaction in the strongly coupled regime characterized by large ion fluxes and the capture of particles released from the surface in the interaction region. MAGNUM-PSI will use expanding hydrogen arc plasma in combination with RF heating to yield ITER-relevant fluxes. A pilot issue of MAGNUM-PSI (Pilot-PSI) is in operation and provides experimental results demonstrating the production of a plasma jet with high particle and power flux density [1]. This work presents the results from simulations of a hydrogen plasma and neutrals performed by means of the B2–EIRENE code package for a set of conditions expected in MAGNUM-PSI.

## 2. The B2–EIRENE simulation

The heating chamber of MAGNUM-PSI considered in the simulations is presented schematically in Fig. 1. Cylindrical symmetry is assumed. The plasma jet with a radius of ∼5 cm enters at $y = 0$

* Corresponding author. Fax: +49 3834 554301.
*E-mail address:* baeva@inp-greifswald.de (M. Baeva).

0022-3115/$ - see front matter 
doi:10.1016/j.jnucmat.2007.01.029

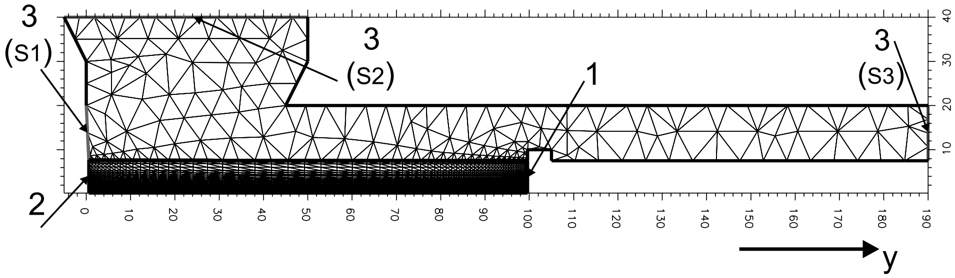


Fig. 1. Schematic view of the working chamber in MAGNUM-PSI and the B2 and EIRENE computational grids: 1 – target, 2 – plasma inlet, 3 – pump.

and streams towards the target plate positioned at $y = 100$ cm. The plasma is confined by a magnetic field of ~3 T. The plasma is studied on the basis of the 2D fluid code B2 [2]. The plasma density, electron and ion temperature have a normalized radial profile at the inlet (Fig. 2) and a fixed peak value. The derivative of the parallel flow velocity is set to zero. Neutral gas flow ($H_2$), uniformly distributed, is introduced at the inlet. Additional gas-puff through the middle of the target can be also considered. Sheath boundary conditions are used at the target assuming $V_y \geqslant C_s$, and energy transmission factors of 4.0 and 2.5 for electrons and ions, respectively. At the wall side of the B2-grid a decay length of 1 cm for all quantities is assumed. Along the axis of symmetry of the working chamber, zero radial gradients are imposed. Heat flux and momentum flux limits are applied with factors of 0.2 and 0.5, respectively. The radial transport coefficients are assigned anomalous values. A diffusion coefficient of $D_i = 0.5$ m$^2$/s, radial thermal conductivities $\kappa_{e,i}/n_{e,i} = 1$ m$^2$/s, and ion viscosity $\eta_i/m_i n_i = 0.2$ m$^2$/s are used in the simulations. The plasma description is self-consistently coupled to the transport of neutrals simulated using the 3D Monte Carlo solver EIRENE [3,4]. The multispecies neutral transport code EIRENE, widely applied in international controlled nuclear fusion devices, solves linear kinetic transport equations for almost arbitrary geometrical complexity and a given plasma background. It uses external databases for atomic, molecular, spectral, and for surface interaction data. The neutral–plasma reactions used in this study are listed in Table 1. In EIRENE the ground state atoms and molecules are followed. The excited atomic and molecular states are accounted for in terms of effective rate coefficients of collisional and radiative processes which are calculated prior to the transport simulation by means of a collisional–radiative model [5]. Neutrals are produced due to plasma recycling and by volume recombination. Additionally, neutral molecules are injected at the plasma inlet (Fig. 1). The interaction of the neutrals with the surfaces of the device is described by an albedo of unity for all surfaces except those where pumps are considered. Atoms are reflected according to

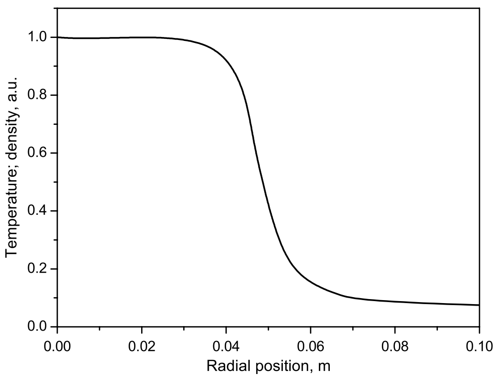


Fig. 2. Specified radial profile of the electron and ion temperature and plasma density.

Table 1
List of the reactions considered in the EIRENE simulation

| | Reaction |
|---|---|
| Molecule–plasma | $e + H_2 \rightarrow H + H + e$ |
| | $e + H_2 \rightarrow H_2^+ + 2e$ |
| | $e + H_2 \rightarrow H^+ + H + 2e$ |
| | $H^+ + H_2 \rightarrow H + H_2^+$ |
| | $H^+ + H_2 \rightarrow H^+ + H_2$ |
| Atom–plasma | $e + H \rightarrow H^+ + 2e$ |
| | $H^+ + H \rightarrow H + H^+$ |
| Bulk ion–plasma | $e + H^+ \rightarrow H + h\nu$ |
| | $e + e + H^+ \rightarrow H + e$ |
| Test ion–plasma | $e + H_2^+ \rightarrow 2H^+ + 2e$ |
| | $e + H_2^+ \rightarrow H^+ + H + e$ |
| | $e + H_2^+ \rightarrow H + H$ |

results from TRIM Code calculations. All other fluxes from surfaces are in form of thermal molecules.

## 3. Results

The cases considered in the simulation are summarized in Table 2. The electron temperature at the plasma inlet has a peak value of 12 eV in cases 1–5 and 15 eV in case 6. The ion temperature peak value at the inlet in all cases is 2 eV. A neutral gas flow of hydrogen molecules is introduced at the plasma inlet with rates ($\phi_{in}$) varied between (1–5) slm and an initial molecule temperature of 2 eV. For cases 4 and 5, neutral molecules with temperatures of 0.026 eV and flow rate ($\phi_{tg}$) of 1 slm are fed through the middle of the target. Further, the surface albedo ($A_s$) of surfaces S1, S2 and S3 (see Fig. 1) is varied to obtain different conditions in front of the target.

Fig. 3 shows the axial distribution of the electron (a) and ion (b) temperature, and the electron density (c) in the working chamber of MAGNUM-PSI. In all cases, the electron temperature decreases towards the target and has values in the range (2–4) eV except in case 5, where a value below 1 eV is observed. The ion temperature increases beyond the inlet due to equilibration between electrons and ions and decreases further to almost the same values as the electron temperature in front of the target. The plasma density is peaked at $y \sim 95$ cm and reaches values from $\sim 4 \times 10^{13}$ cm$^{-3}$ up to $\sim 5 \times 10^{14}$ cm$^{-3}$. Beyond this point the plasma density decreases significantly. In all cases a formation of an ionization front in front of the target can be observed.

Table 2
Cases considered for the simulations

| Case | 1 | 2 | 3 | 4 | 5 | 6 |
|---|---|---|---|---|---|---|
| $T_e$ (eV) | 12 | 12 | 12 | 12 | 12 | 15 |
| $T_i$ (eV) | 2 | 2 | 2 | 2 | 2 | 2 |
| $\phi_{in}$ (slm) | 1 | 2 | 2 | 5 | 5 | 2 |
| $\phi_{tg}$ (slm) | – | – | – | 1 | 1 | – |
| $A_s$ (S1) | .99 | .9 | .99 | .9 | .99 | .99 |
| $A_s$ (S2) | .99 | .9 | .99 | .9 | .99 | .99 |
| $A_s$ (S3) | .95 | .9 | .99 | .9 | .95 | .90 |

Fig. 4 presents the axial profiles of the plasma pressure (a), the ion flux density (b), and the plasma heat flux density (c). The plasma pressure, having values (70–400) Pa in the different cases, remains almost constant along the axis and drops in front of the target. Similar behavior shows the plasma heat flux density. Along the distance from the inlet to the target it has almost constant values in the range (1–11)MW m$^{-2}$ and drops in front of the target. Hence, a detached plasma regime is obtained. The particle flux density of the hydrogen ions reaches values about $10^{24}$ m$^{-2}$ s$^{-1}$ at the target.

To get a better understanding of the results obtained, the processes for case 3 are considered in more detail in what follows. In that case the input plasma power is ~30 kW, and the total energy content of 1.03 J is distributed as 0.44 J and 0.59 J between the electrons and ions, respectively. The axial profiles of the source terms (the product of the corresponding densities and the rate coefficient) for ionization, dissociation, molecular and atomic ion recombination obtained for case 3 (see Table 2) are shown in Fig. 5(a). Fig. 5(b) presents the axial

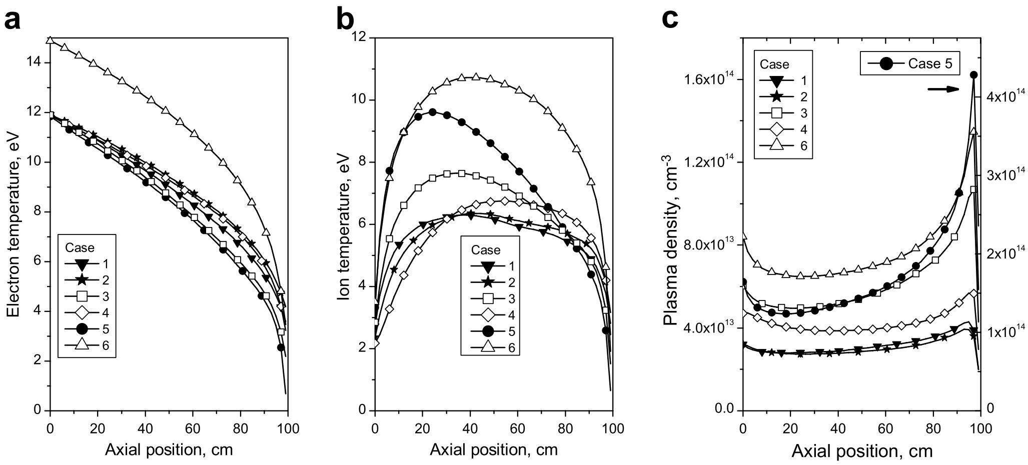


Fig. 3. Axial profiles of the electron temperature (a), ion temperature (b), and the electron density (c).

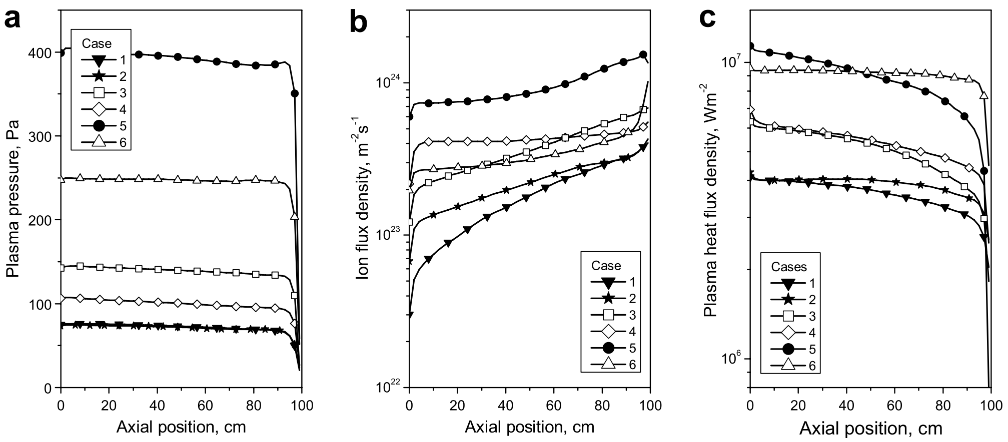


Fig. 4. Axial profiles of the plasma pressure (a), ion flux density (b), and the plasma heat flux density (c).

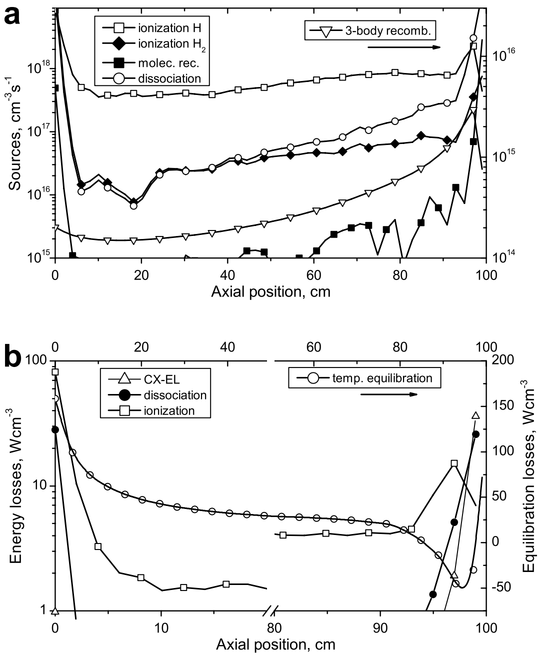


Fig. 5. Axial profiles of (a) the sources for ionization, dissociation, atomic and molecular recombination, and (b) the energy losses due to ionization, dissociation, charge exchange and elastic collisions, and temperature equilibration in case 3.

profiles of the electron and ion energy loss rates. Near the plasma inlet ($y \sim 3$ cm), the electrons lose energy mainly due to ionization and dissociation of the incoming neutrals, and temperature equilibration with the ions. The ion temperature increases and reaches a value of $\sim$8 eV at $y \sim 20$ cm (see Fig. 3(b)). Toward the target the ionization losses are lower than the temperature relaxation losses by a factor of $\sim$4–5. From about the middle of the distance, the ionization losses increase again and the plasma density grows. An ionization front builds. About 10 cm far from the target, the energy losses due to ionization and dissociation of the neutrals from plasma recycling increase rapidly. The electron temperature values of $\sim$2 eV and plasma density of $1 \times 10^{14}$ cm$^{-3}$ are observed. The ion energy losses due to charge exchange and elastic collisions increase by a factor of $\sim$30 at $y \sim 5$ cm far from the target. The density of the test ion $H_2^+$ reaches a peak value of $\sim 2.7 \times 10^{13}$ cm$^{-3}$. Consequently, the sources for molecular recombination dominate over the 3-body recombination of the atomic ion. This all shows the effective capture of the neutrals in the working chamber of MAGNUM-PSI. It is worth noting, that in the case of ITER simulations the 3-body recombination dominates. This difference can be explained by the higher values of the molecule density and the electron temperature in the case of MAGNUM-PSI compared with ITER.

## 4. Conclusion

In the present study of the linear device MAGNUM-PSI, several cases varying in gas-puffing and pumping rate, and plasma parameters are simulated with the B2–EIRENE code package to investigate the plasma and neutrals behavior in front of the target. The results obtained show in all cases the formation of an ionization front due to re-ionization of recycled neutrals. This shows the effective capture of neutrals in the heating chamber of MAGNUM-PSI. The plasma density increases considerably for higher neutral pressure values (controlled by gas-puffing or pumping rates) and reaches values of $(1–5) \times 10^{14}\,cm^{-3}$. The calculated particle and energy fluxes for the ions to the target are about $10^{24}\,m^{-2}\,s^{-1}$ and several $MW\,m^{-2}$, respectively. The total plasma heat flux density has values above $10\,MW\,m^{-2}$. It is significantly reduced in front of the target since the electrons and ions are cooled due to ionization and dissociation of $H_2$ molecules, and charge exchange/elastic collisions. The recombination losses near the target are preliminary due to the molecular activated recombination. 3-body recombination of atomic ions plays a minor role at the conditions under investigation, in contrast to ITER, where the 3-body recombination dominates.

## Acknowledgments

This work, supported by the European Communities under the contract of Association between EURATOM/FOM, was carried out within the framework of the European Fusion Programme with financial support from NWO. The views and opinions expressed herein do not necessarily reflect those of the European Commission.

## References

[1] G.J. van Rooij, V.P. Veremiyenko, T.W. Versloot, et al., in: Proceedings of the XXVIIth ICPIG, Eindhoven, Netherlands, July, 2005, p. 18.
[2] B.J. Braams, Computational Studies in Tokamak Equilibrium and Transport, PhD Thesis, University of Utrecht, 1986.
[3] D. Reiter, M. Baelmans, P. Börner, Fus. Sci. Technol. 47 (2) (2005) 172.
[4] D. Reiter, EIRENE – A Monte Carlo linear transport solver, <www.eirene.de>.
[5] K. Sawada, T. Fujimoto, J. Appl. Phys. 78 (1995) 2915.